Research Article | Vol. 28, No. 2 / 20 January 2020 / Optics Express 2466
Optics EXPRESS

20-mJ, sub-ps pulses at up to 70 W average power from a cryogenic Yb:YLF regenerative amplifier

UMIT DEMIRBAS,[1,2,*] HUSEYIN CANKAYA,[1,3] YI HUA,[1,3] JELTO THESINGA,[1] MIKHAIL PERGAMENT,[1] AND FRANZ X. KÄRTNER[1,3,4]

[1]Center for Free-Electron Laser Science, Deutsches Elektronen-Synchrotron DESY, Notkestraße 85, 22607 Hamburg, Germany
[2]Laser Technology Laboratory, Department of Electrical and Electronics Engineering, Antalya Bilim University, 07190 Dosemealti, Antalya, Turkey
[3]Physics Department, University of Hamburg, Luruper Chaussee 149, 22761 Hamburg, Germany
[4]The Hamburg Centre for Ultrafast Imaging, Luruper Chaussee 149, 22761 Hamburg, Germany
*uemit.demirbas@cfel.de

Abstract: We report, what is to our knowledge, the highest average power obtained directly from a Yb:YLF regenerative amplifier to date. A fiber front-end provided seed pulses with an energy of 10 nJ and stretched pulsewidth of around 1 ns. The bow-tie type Yb:YLF ring amplifier was pulse pumped by a kW power 960 nm fiber coupled diode-module. By employing a pump spot diameter of 2.1 mm, we could generate 20-mJ pulses at repetition rates between 1 Hz and 3.5 kHz, 10 mJ pulses at 5 kHz, 6.5 mJ pulses at 7.5 kHz and 5 mJ pulses at 10 kHz. The highest average power (70 W) was obtained at 3.5 kHz operation, at an absorbed pump power level of 460 W, corresponding to a conversion efficiency of 15.2%. Despite operating in the unsaturated regime, usage of a very stable seed source limited the power fluctuations below 2% rms in a 5 minute time interval. The output pulses were centered around 1018.6 nm with a FWHM bandwidth of 2.1 nm, and could be compressed to below 1-ps pulse duration. The output beam maintained a TEM_{00} beam profile at all power levels, and possesses a beam quality factor better than 1.05 in both axis. The relatively narrow bandwidth of the current seed source and the moderate gain available from the single Yb:YLF crystal was the main limiting factor in this initial study.

1. Introduction

Yb:YAG gain media possesses a room-temperature (RT) fluorescence lifetime (τ) of 940 µs, and an emission cross section (σ_{em}) of around 2.15 x10^{-20} cm^2, resulting in a relatively large $\sigma_{em}\tau$-product of 2×10^{-23} cm^2s [1]. Moreover, it is thermo-mechanically quite strong, enabling different laser gain geometries such as crystalline fibers [2], or thin disks [3,4]. As a result, it become the material of choice in the development of high-power and high-energy laser/amplifier systems [3–9]. Furthermore, the thermo-opto-mechanical properties of Yb:YAG are improved further by cooling to cryogenic temperatures (e.g: $\sigma_{em}\tau$-product increase ~4.5 fold, thermal conductivity increases ~4 fold, thermal expansion reduces ~3 fold) [10–12]. Unfortunately, the main drawback of Yb:YAG media is its narrow and steep gain profile, for details see Fig. 1 in [1]. The gain bandwidth of Yb:YAG at room temperature (RT) has a full-width-half-maximum (FWHM) of 8 nm, which narrows down to a 1.5 nm at cryogenic temperatures. As a result, gain-narrowing effects are hard to compensate, and the achievable pulsewidth upon amplification is usually limited around 1 ps at RT, and a few picoseconds at cryogenic temperatures.

As a promising alternative to Yb:YAG, the Yb:YLF gain medium is known to exhibit broader emission bands even at cryogenic temperatures [13–16]. The uniaxial Yb:YLF material, possesses

#384968 https://doi.org/10.1364/OE.384968
Journal © 2020 Received 3 Dec 2019; revised 3 Jan 2020; accepted 7 Jan 2020; published 16 Jan 2020

Optics EXPRESS

a gain bandwidth of 10 nm for the E//a axis at cryogenic temperatures [1]. Moreover, unlike Yb:YAG, the emission profile is rather smooth, which minimizes gain-narrowing effects, that could potentially enable amplification of sub-250 fs long pulses. At the same time, parameters of Yb:YLF such as thermal conductivity, thermal expansion coefficient, thermo-optic coefficient (dn/dT) are better than for RT Yb:YAG. On the other hand, the emission cross section of Yb:YLF at 80 K is only around 0.7×10^{-20} cm^2 for the E//a axis, which is around 3 times lower than RT-Yb:YAG and 14 times lower when compared to cryogenic Yb:YAG. However, the longer fluorescence lifetime, τ=1990 μs [17], partly balances for the reduced gain, resulting in a $\sigma_{em}\tau$-product of 1.4 x10^{-23} cm^{2}s in comparison with 2×10^{-23} cm^{2}s and 9.4×10^{-23} cm^{2}s of RT and cryogenic Yb:YAG, respectively. As a result of the low emission cross section, one also suffers from a rather high saturation fluence (14 J/cm^2) in Yb:YLF, which creates challenges in optimizing extraction from amplifiers. As an example, for a stretched pulsewidth of 1 ns, the cavity optics has an estimated laser induced damage threshold (LIDT) of around 6.3 J/cm^2, and long-term damage free operation usually requires operating the amplifier at a lower/safer value of ~3 J/cm^2 or below. Operating the amplifier at a fluence value much lower than the saturation fluence: (i) reduces the extraction efficiency of the circulating amplified pulse, (ii) increases output energy fluctuations upon undesired perturbations, and (iii) results in circulation of a Gaussian beam profile in the amplifier (which is known to have 2 times higher fluence compared to flattop beams). Note that, despite these disadvantages, if the amplifier is operated at repetition rates much higher than $1/\tau$ (~500 Hz for Yb:YLF), via employing effective cumulative extraction with many pulses, the above issues are partially resolved.

Several groups have successfully demonstrated amplification with Yb:YLF gain media at cryogenic temperatures [18–21]. In their pioneer work, using a regenerative amplifier (regen) pumped with 4-ms, 100-W pump pulses at 20 Hz, Kawanaka et al. demonstrated amplification of 20 pJ pulses from a Ti:Sapphire laser to 30 mJ (600 mW average output power) [18]. Output pulses were centered around 1018 nm and could be compressed down to 800 fs duration [18]. The pulse energies achieved in [18] were reported as being limited by LIDT (1.7 mm beam diameter, 2.7 J/cm^2 peak fluence) [18]. Later, by using a 1.75 mm thick 25% Yb:YLF crystal as the gain medium, Rand et al. demonstrated amplification of nJ-pulses to 1 mJ energy at repetition rates up to 10 kHz (10 W average power) [19]. The system was pumped by a 50-W, 940-nm fiber coupled pump source, and a rather tight spot size diameter of 0.5 mm was used for efficient (~20%) extraction at a peak fluence of 1 J/cm^2 [19]. Later, this regen was used as a seed for a cryogenic Yb:YLF 8-pass amplifier to boost the pulse energy from 1 mJ to 10 mJ, and the corresponding average output power reached 100 W [20]. In the 8-pass amplifier system, two 1%-doped 8 mm long Yb:YLF crystals were pumped by a 350-W, 960-nm fiber coupled diode, and a pump spot diameter of 1.6 mm was employed (peak fluence: 1 J/cm^2, o-to-o efficiency: 25.7%) [20]. The output pulses were centered around 1018 nm, and could be compressed down to 700-fs duration [20]. Recently, pulse energies up to 190 mJ were reported at 10 Hz, from a three stage Yb:YLF amplifier system, consisting of one regenerative and two 4-pass amplifiers [22]. In all of the amplification studies discussed above, the E//a axis of the Yb:YLF gain medium showing a broad emission spectrum were selected. As an alternative, Manni et al. illustrated amplification of a cw seed source from 2.6 mW to 40 W power in a cryogenic multipass Yb:YLF amplifier employing the strong and narrow gain line at 995 nm in the E//c axis of the amplifier medium [21]. The system was pumped at 960 nm with a pump spot diameter of 1.2 mm, and an optical-to-optical conversion efficiency above 50% was achieved [21]. Note that amplification of a cw seed rather than ultrashort pulses enables optimization of efficiencies by tight focusing, which is not possible in ultrashort pulse amplification due to LIDT issues.

Here, we report direct generation of 20-mJ pulses at repetition rates up to 3.5 kHz, and with a corresponding average power up to 70 W from a cryogenic Yb:YLF regenerative amplifier. For pumping, the output of a 960-nm fiber coupled diode-module was imaged to a pump spot

Optics EXPRESS

diameter of 2.1 mm inside a 2 cm long 0.5% Yb-doped Yb:YLF crystal. Stretched (1-ns) pulses with 10 nJ energy from a Yb-fiber front-end system were used as the seed source. Amplification of the 10-nJ seed pulses to the 20 mJ level was demonstrated at repetition rates ranging from 1 Hz to 3.5 kHz. The output pulse energy was kept at a very safe energy level of 20 mJ, i.e. a peak fluence level of ~1.15 J/cm^2, to obtain a long-term stable system that is far away from LIDT of optics. Pulse energies of 10 mJ, and 5 mJ were further obtained at higher repetition rates of 5 kHz and 10 kHz, respectively. The optical spectrum of the amplified pulses was centered around 1018.6 nm with a FWHM bandwidth of 2.1 nm, which enabled compression of the pulses below 1 ps in duration.

The paper is organized as follows. Section 2 provides details on the experimental setup. In section 3, we present the experimental results, first on characterization of the unseeded regenerative amplifier via cw-lasing experiments, and later on amplification results with seeding. We finalize the paper with a brief conclusion in Section 4.

2. Experimental setup

Figure 1 shows a schematic of the cryogenic Yb:YLF regenerative amplifier that is used in the experiments. The laser diode module supplied up to 2 kW of output power at a central wavelength of 960 nm, from a 600 μm core diameter fiber, and the pump beam had an estimated M^2 of 220. In the regenerative amplification studies, the gain medium was pulse-pumped with 50 μs pulses at 5-10 kHz, with 100 μs pulses at 2.5-3.5 kHz, with 150 μs long pulses at 1 kHz, and with 1 ms long pulses at lower repetition rates. The pump light was first collimated (f1:72 mm), and then focused (f2:250 mm) to a pump spot diameter of 2.08 mm (~2.1 mm). Due to the small working-range of the f1-f2 telescope, another lens (f3) with a focal length of 150 mm was used in 2f-2f geometry to re-image the pump beam inside the gain medium. The 2-cm long, 0.5% Yb-doped Yb:YLF crystal had 3-mm long undoped endcaps diffusion-bonded on both ends to minimize surface deformations under thermal load (a total crystal length of 26 mm). The nearly c-cut sample enabled usage of the broadband E//a axis in lasing/amplification experiments. Note that, the c-axis was oriented 10° away from the direction of propagation to create some natural birefringence to minimize depolarization losses [see Fig. 1(b) in [20] for the sketch of crystal orientation]. The surfaces of the crystal, as well as the windows used on the dewar contained antireflection coatings that were effective both at the pump and laser wavelengths. The crystal was indium bonded from the top side to a cold head, which was cooled to cryogenic temperatures by liquid nitrogen. The bow-tie type regenerative ring cavity consisted of two dichroic mirrors (DM) with a radius of curvature of 20 m, and two flat high reflectors. The distance between the curved mirrors was set to 75 cm length, and the total cavity length was around 3 m, corresponding to a cavity round-trip time of around 10 ns and a repetition rate of about 100 MHz. Two thin-film polarizer's (TFPs), a half-wave plate (HWP) and a Pockell cell (PC) with a rise time of 6 ns were used for seeding of the amplifier (TFPs and HWP were antireflection coated at 1030 nm, whereas the PC AR coating was optimized for 1020 nm). The system is seeded by stretched (ns) pulses with 10 nJ energy from a fiber front-end, and the details of the seed source can be found in [23]. The cold cavity had a calculated beam diameter of 2.23 mm and 2.15 mm at the center of the Yb:YLF crystal and PC, respectively. Under pumping conditions (~350 W absorbed power), and an estimated thermal lens of around + 10 m, the beam size shrinks to 2.08 mm and 1.92 mm, at the center of the Yb:YLF crystal and PC, respectively. We refer the readers to the experimental section of [1] for a more detailed discussion on properties of the pump diode used in this study.

Optics EXPRESS

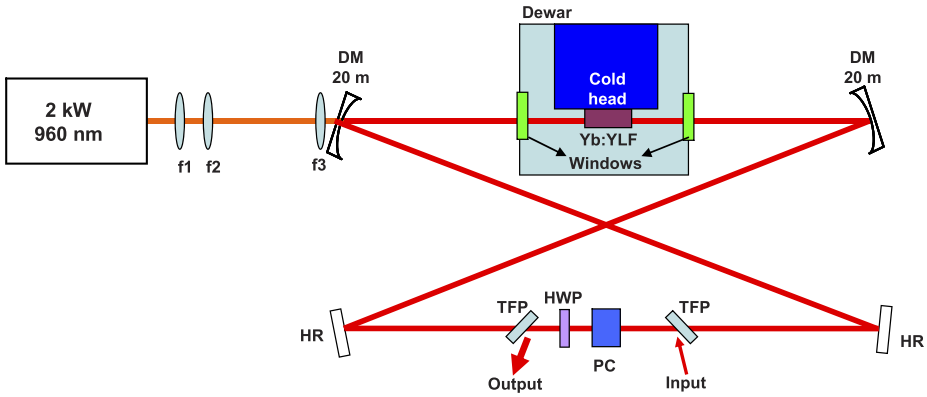

Fig. 1. Schematic of diode pumped cryogenically cooled Yb:YLF regenerative amplifier. DM: Dichroic mirror, HR: High reflector mirror, f1-f3: pump beam optics/lenses, PC: Pockell cell, TFP: Thin-film polarizer, HWP: Half-wave plate.

3. Experimental results

3.1. Continuous-wave and quasi continuous-wave lasing results

Figure 2(a) shows the continuous-wave lasing results at 20% effective output coupling, where the results of the regenerative laser cavity are compared with a simple short-cavity setup. The short cavity results have been described in detail in [1], where a flat-flat cavity with a total length of 20 cm was used. Here the regenerative laser cavity results are taken with the cavity shown in Fig. 1, but without the PC implemented. Also, the rotation angle of the HWP is modified, and the two TFP surfaces provided output coupling, and the total power of the two output beams is measured. For the short-cavity, we have observed a lasing threshold of 60 W, a slope efficiency of 66%, and achieved up to 305 W of output power at an absorbed pump power of 510 W [1]. In comparison, the regenerative laser cavity had a measured cw-lasing threshold of 90 W and a slope efficiency of 58%. Moreover, the maximum cw output power was limited to 230 W at an absorbed pump power of 505 W. Note that, in both cases, due to the onset of thermal effects [1], pumping the system with an average power above 500 W did not provide further increase in output. We believe that this restraint is a result of boiling liquid nitrogen boundary condition, where the Leidenfrost effect limits the heat extraction coefficients to around 10 kW/Km^2 at the LN_2 boundary [47-49]. Basically, once the system generates a heat load that is above a critical level, an insulating nitrogen gas forms at the LN_2 boundary, cuts down the thermal contact, and as a result the Yb:YLF crystal starts to heat up rapidly. We have experimentally found out that, in our current system, this effect starts for an absorbed pump power of around 500 W in the case of efficient lasing/amplification, and the process arouses earlier when optical efficiency is lower. In future work, usage of better engineered heat extraction systems could improve the thermal limits that have been observed in this initial study.

When we compare the short cavity and regenerative laser cavity results [Fig. 2(a)], we clearly see that the increased losses of the regenerative laser cavity compared to the short-cavity (due to the insertion of TFPs and HWP) has raised the lasing threshold. To be more specific, using the seed laser, we have determined the single-pass loss of the short and regenerative laser cavity (without the PC) at around 3% and 5%, respectively. Moreover, in the case of the regenerative laser cavity, the output laser beam had a TEM_{00} beam profile and an M^2 below 1.05 at all power levels. In contrast, the short cavity with flat-flat mirrors allowed for higher order modes, and had a flat-top beam profile with an M^2 of 2.5 at the 300 W power level. Hence, the mode-matching between the multi-mode pump beam and the intracavity laser mode is expected to be better in

Optics EXPRESS

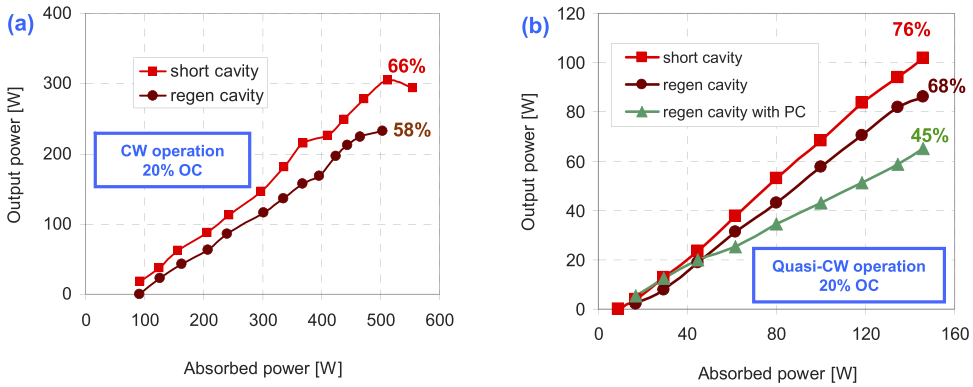

Fig. 2. Measured cw (a) and quasi-cw (b) laser performance of the cryogenic Yb:YLF laser at an output coupling value of 20%. Short cavity corresponds to a simple 20 cm long flat-flat cavity, containing a flat dichroic mirror and a flat output coupler [1]. Regenerative amplifier (regen) cavity is described in detail in Fig. 1. Regen cavity laser performance data with and without the pockell cell (PC) is shown in (b). Results of the short-cavity are reproduced with permission from [1].

the short-cavity, at the expense of reduced beam quality. The regenerative laser cavity results (especially the slope efficiency achieved) show that, despite the single-mode intracavity laser beam, the mode-matching to the pump mode is still quite good, which is important for efficient energy extraction in the later amplification studies.

To elaborate on the issue in more detail, Fig. 2(b) shows the measured quasi-cw (long pulse) laser performance of the Yb:YLF laser, where short cavity, regenerative cavity and regenerative cavity with PC results are compared to each other. The results are taken again using a 20% output coupling, but this time with pulsed pumping of the system with 10 ms long pump pulses at 10 Hz. First of all, we see that the slope efficiency improves, due to the lower thermal load on the crystal. This shows that, even though the obtained cw efficiency curves were rather linear in Fig. 2(b), thermal effects were already present. Also with the insertion of the Pockels cell in the cavity, the passive losses increased, which reduced the slope efficiency and the obtainable output power from the system. To confirm this, we measured the losses of the regenerative cavity (including the PC) as 8%. Note, this loss level contains passage of the beam through the Yb:YLF crystal, two TFPs, one HWP, two dewar windows, two 20 mm long BBO crystals and 2 protective windows in the PC, amounting to 20 antireflective surfaces (in contrast, the losses of the high-reflective coatings can be ignored). Unfortunately, some of the AR coatings employed were not as good as desired in this initial study, and in future work, we hope to suppress the cavity losses below 5%. We also note that, these are the loss levels of the cold/un-pumped cavity. We believe that the effective loss level under pumping is higher, due to aperture effects caused by thermally induced beam pointing in the one-side cooled Yb:YLF crystal (e.g. soft aperture on Yb:YLF crystal, and hard aperture on PC).

In summary, the lasing results clearly underline the importance of minimizing losses for efficient lasing/amplification, especially while employing the lower-gain E//a axis of Yb:YLF gain medium. The results also highlight the presence of thermal effects and its role in lowering system efficiency. We have also seen that, for this specific system, due to the limited cooling efficiency of the liquid nitrogen boundary, the absorbed pump power applied to the system is limited to about 500 W. We refer the reader to the literature for more detailed discussions of lasing performance of Yb:YLF lasers in the cw [13,24–29], quasi-cw [30–34], Q-switched [14,29] and cw mode-locked [35,36] regimes.

Optics EXPRESS

3.2. Regenerative amplification results

In this subsection, we discuss the regenerative amplification results. During the experiments, we extracted 20 mJ energy from the regenerative amplifier at repetition rates between 1 Hz and 3.5 kHz. The output energy is kept at 20 mJ, to enable long-term stable operation, far away from LIDT of optics. On the other hand, for short time scales, the system was operated at higher energy levels of up to 35 mJ, and no damage was observed. At repetition rates higher than 3.5 kHz, due to the reduced gain per pulse and the onset of thermal effects, the average power was limited to around 45-70 W. Hence, the obtainable energies were below 20 mJ (10 mJ at 5 kHz, 6.5 mJ pulses at 7.5 kHz and 5 mJ pulses at 10 kHz). Note that, the specified deviation in extractable average power of the system (45-70 W level) was due to day-to-day variations of passive losses and cavity alignment of the initial prototype system, and could be improved with further engineering. In the following, as a representative example, we will first present details of the amplification results taken at 2.5 kHz. Later, we also present amplification results at 3.5 kHz, which was the highest repetition rate where we achieved output energies of 20 mJ. We will finalize the section, by presenting amplification results at 10 kHz, which is the highest repetition rate we operated the system due to the limited capabilities of the PC driver electronics at hand.

Figure 3(a) shows the measured regenerative amplifier output power as a function of absorbed pump power at a repetition rate of 2.5 kHz. While taking the data in Fig. 3(a), the number of round-trips (n) in the regen amplifier was set to 70, and the seed energy was 10 nJ. The crystal was pulse-pumped using pump pulse durations of 100 microseconds (25% duty cycle), where the pump pulse duration corresponds to only 1/20th of the Yb:YLF upper state lifetime. The regenerative amplifier produced 51.7 W of average power, at an absorbed pump power of 320 W (incident power = 430 W, with 75% absorbed). The corresponding efficiency of the system in terms of incident and absorbed pump power are then around 12% and 16.2%, respectively. The trend in Fig. 3(a) clearly shows that, extraction of higher energies (output power) from the system is feasible and only limited by the LIDT of cavity optics. Note that, the pulses are amplified from about 5 nJ to 20 mJ in 70 round-trips (5 nJ is the estimated in-band seed energy, see Fig. 5). Hence, the corresponding overall amplification is around 4×10^6, and the average net amplification per pass in then around 1.24 (considering 8% losses, the average amplification of the Yb:YLF medium is 1.32 in each pass). Of course, this is an average amplification value, in the real amplifier, gain per pass will be lower towards the final round-trips due to cumulative saturation of the gain at higher repetition rates.

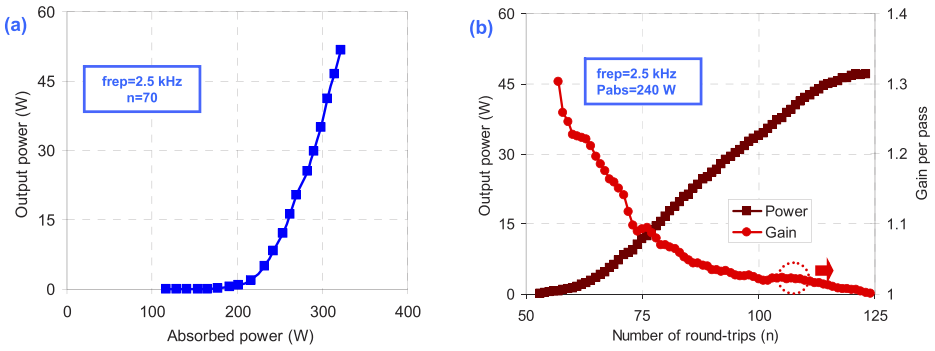

Fig. 3. (a) Variation of regenerative amplifier average output power with absorbed pump power at a repetition rate of 2.5 kHz. The data is taken at a round-trip number n = 70. (b) Variation of regenerative amplifier average output power as a function of number of round-trips in the amplifier (n), at a fixed absorbed pump power of 240 W. Variation of single pass gain is also shown for this case.

Optics EXPRESS

Figure 3(b) on the other hand shows the change in regenerative amplifier output power as a function of round trips in the amplifier, at a fixed average absorbed pump power of 240 W (310 W incident pump power). As we can see from Fig. 3(b), due to the reduced gain at the lower absorbed pump power level, the amplifier requires more round-trips (124) to reach the desired energy range. Specifically, the output energies and output power were limited to 18.9 mJ and 47 W level 124 round-trips (pumping with 15 W higher power easily enables 20 mJ level pulses). The corresponding overall amplification and average net amplification per pass were around 3.78×10^6 and 1.13, respectively. Note that, Fig. 3(b) also shows the measured additional gain per pass in the amplifier, where we initially start with gains of around 1.3 for each additional pass (around $n = 50$), and we later saturate at a net gain of almost 1. This clearly shows the saturation behavior of the amplifier, which could also be used to reduce intensity fluctuations in output energy (note, here saturation is observed as a result of the interaction of many consecutive pulses). Moreover, operating at lower absorbed pump power levels reduces thermal effects and increases the stability of the cavity. In addition, for this case, the efficiency of the system in terms of incident and absorbed pump power was slightly higher and were around 19.6% and 15.2%, respectively. On the other hand, compared to the case in Fig. 3(a), the reduced pump power lowers the gain, increases the required number of passes, and increases the overall B-integral of the beam from around 1.2 to 1.7. We note that, despite this, for both cases, the beam quality and the intensity stability of the regenerative amplifier were quite good, as it will be discussed in more detail below.

In the following, we provide additional information about other relevant parameters of the Yb:YLF regenerative amplifier such as optical spectrum, output beam quality and output power stability. Figure 4, shows the measured temporal dynamics of the amplifier. The oscilloscope trace shown in Fig. 4 was acquired using two separate fast (GHz) Si photo-detectors, where one detector was used to monitor the intracavity pulse energy, and the second detector was used to observe the output beam energy. The data is taken at 2.5 kHz, under the same conditions as were used in Fig. 3(a). The intracavity regen signal (shown in green), clearly exhibits gradual amplification of the pulse after each pass, where the pulse energy after 50, 60 and 70 rounds trips are indicated. Note that, the output pulse trace, that is shown in yellow, has some spikes after the main pulse. While adjusting the timing of the exit pulse, we saw that these additional spikes are not real pulses and occur due to ringing of the detector. The response time of the PC (6 ns) was short enough to provide clean output pulses with contrast ratios better than 20:1.

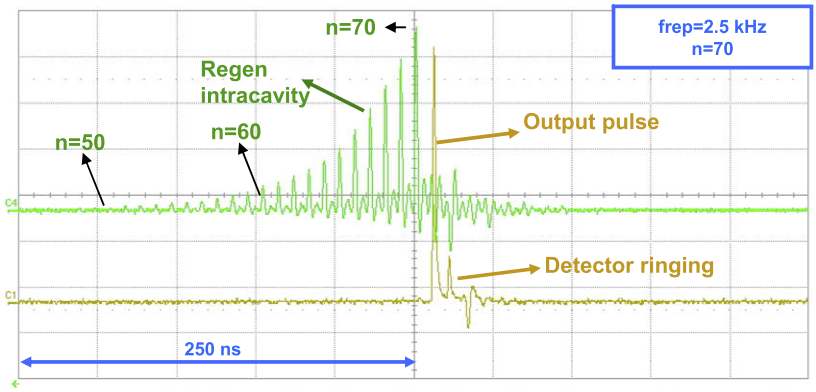

Fig. 4. Measured time dynamics of the Yb:YLF amplifier using two fast photodiodes. The data is taken at an output pulse energy of 20 mJ, at a pulse repetition rate of 2.5 kHz and at an absorbed pump power level of 320 W. Dynamics of the intracavity circulating pulse (green) as well as the amplified output pulse (yellow) are shown.

Optics EXPRESS

The optical spectrum of the seed and amplified pulses are shown in Fig. 5, along with the measured emission cross section profile of the Yb:YLF gain medium for the E//a axis. The seed spectrum was centered around 1019.5 nm and had a FWHM of 2.2 nm. The spectra of the amplified pulses were shown at pulse energies of 4 and 20 mJ. It is clear that, the seed central wavelength was not optimum, and hence the sharp gain edge of Yb:YLF at long wavelengths shifted the center wavelength of the amplified pulses to 1018.65 nm. However, due to the flat gain profile, the FWHM of the amplified pulses still had a width of 2.1 nm. The corresponding transform-limited pulse duration for such a spectrum is around 700-fs, and we have measured a sub-ps pulse duration earlier from a lower repetition rate version of this system [37,38]. On the other hand, it is clear from Fig. 5 that, the current bandwidth of the amplified pulses is mainly limited by the seed source. In our future studies, by developing a broader seed source (FWHM >15 nm), we are hoping to make full use of the relatively flat and broad amplification bandwidth of Yb:YLF covering at least the 1013-1019 nm region, which should result in compressed pulsewidths below 500 fs, and maybe even sub-250-fs in well designed systems (with intracavity/extracavity pulse shaping).

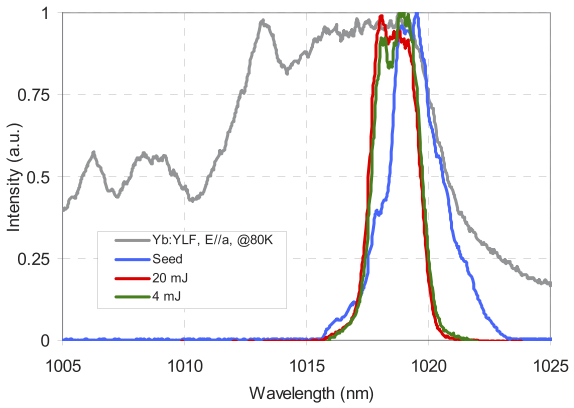

Fig. 5. Optical spectrum of seed pulse and amplified pulse at an output pulse energy of 4 mJ and 20 mJ. The amplified pulses have a FWHM of 2.1 nm centered around 1018.6 nm, that ideally supports 700-fs level pulses. The data is taken at a pulse repetition rate of 2.5 kHz. The measured emission cross section for the E//a axis is also shown in arbitrary units at 80 K.

As mentioned earlier, while discussing the lasing results of the regenerative cavity, the cavity mode selection capability of the system enabled a TEM_{00} output at all output power/energy levels, despite the usage of a highly multimode pump source and presence of thermal effects. To demonstrate that, Fig. 6 shows the measured beam profile of the amplifier output in near field (around 20 cm after the amplifier exit port) and far field (measured at the focus of a 15 cm lens). Both the near-field and far-field measurements confirm the single transverse mode laser beam profile. Note that, the near-field beam profiles also demonstrate slow shrinking of the output beam size, consistent with simulations. From the variation of measured beam size, we have estimated formation of a positive thermal lens of magnitude 10-20 meters within the Yb:YLF crystal (at an average absorbed pump power of around 300 W). We have also measured the M^2 value of the output beam, and as expected we have shown that the beam quality is better than 1.05 in both axis (Fig. 7: data is taken at an output power level of 40 W). Moreover, despite usage of a one-sided cooling geometry, the beam is quite symmetric, with an ellipticity coefficient higher than 0.9, and with an astigmatism below the measurement limits of the system.

We also discuss our amplification results in terms of energy stability. As discussed earlier, due to the low emission cross section in the E//a axis, Yb:YLF has a rather high saturation fluence of

Optics EXPRESS

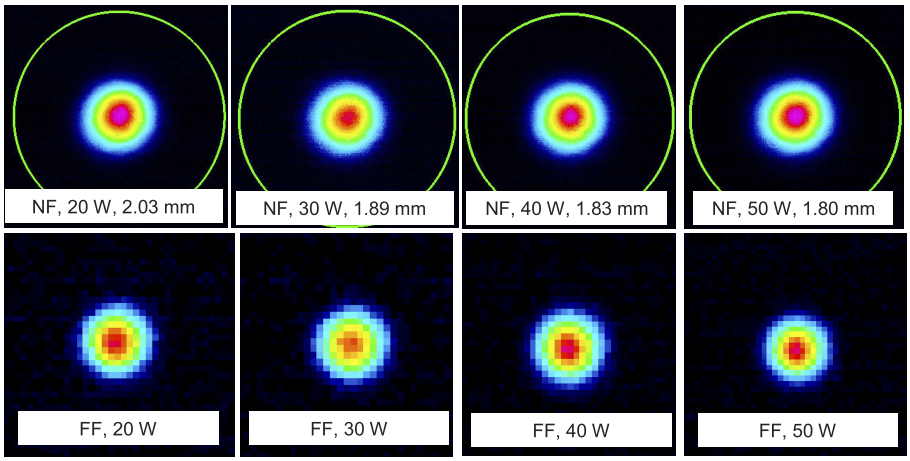

Fig. 6. Measured near field (NF) and far field (FF) beam profiles of the regenerative amplifier at several different output power levels. The data is taken at a pulse repetition rate of 2.5 kHz.

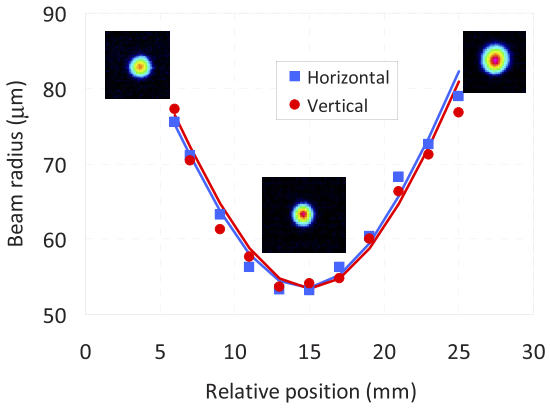

Fig. 7. Measured caustic of the regenerative amplifier at 40 W average power (16 mJ pulses at 2.5 kHz). Beam quality factor (M^2) was estimated to be below 1.05 in both axis.

14 J/cm^2. For the 20 mJ, ~2 mm Gaussian beam, the estimated peak fluence of the intracavity pulse (in the last round-trip) is only around 1.25 J/cm^2, which is much lower than the saturation fluence. As discussed earlier, this creates challenges in optimizing extraction efficiency as well as minimizing output energy fluctuations. On the other hand, note that, at a repetition rate of 2.5 kHz, we have a pulse extracting from the system at every 400 microseconds. Hence, in Yb:YLF gain media that has a fluorescence lifetime (τ) of 2 ms, we have effectively 5 pulses closely interacting with each other during the amplification process, with a total fluence of 12.5 J/cm^2. As a result, operating the Yb:YLF amplifier at a repetition rate much above $1/\tau$ (~0.5 kHz) can be used (i) to enhance extraction efficiency, (ii) and improve energy stability of the system.

Despite the advantages of higher repetition rate operation, it is still beneficial to minimize any perturbations that could cause instability of the amplifier, since the overall gain of the amplifier is quite high (>10^6). Therefore, we use a high stability seed laser system with power stability better than 0.13% rms measured over a 12 minute time interval [ratio of standard deviation in energy to mean energy value, as shown in Fig. 8(a)] [23]. Moreover, the incident pump power stability of the regenerative amplifier was measured to be around 0.12% rms [Fig. 8(b)]. On the other

Optics EXPRESS

hand, due to the shift/fluctuations of diode central wavelength and spectral shape, the variation in absorbed pump power was slightly higher [Fig. 8(c): 0.26%]. Basically, the absorption peak of Yb:YLF around 960 nm is quite narrow (FWHM:~1.75 nm), compared to the spectral width of the current pump module (FWHM: 4 nm). Use of diode modules with improved temperature control can be used to lower the fluctuations in absorption in future studies. Of course, one can also use pump wavelengths of around 940 nm for pumping Yb:YLF systems, where the system is expected to have lower sensitivity to pump wavelength fluctuations due to the much broader absorption profiles. But this comes at the expense of increased quantum defect (from 5.7% to 7.7%) and a lower absorption coefficient, which increases thermal problems. Despite the usage of a wavelength shift sensitive 960 nm pump source in this study, we have measured an average output power fluctuation of only around 1.7% rms from the Yb:YLF amplifier in a 5 minute time interval [Fig. 8(d)]. We note that, this data is taken from a prototype system with an open cavity that is susceptible to air convection. Moreover, water cooling of the cavity elements were not fully implemented, which could further minimize energy fluctuations. Finally, we are also planning to implement an liquid nitrogen auto-refill system to the Yb:YLF Dewar, which is known to be effective in improving long term (hours) stability of the system (this enables a fixed liquid nitrogen level inside the Dewar, and minimizes mechanical/thermal fluctuations of the Yb:YLF crystal and Dewar optics/windows).

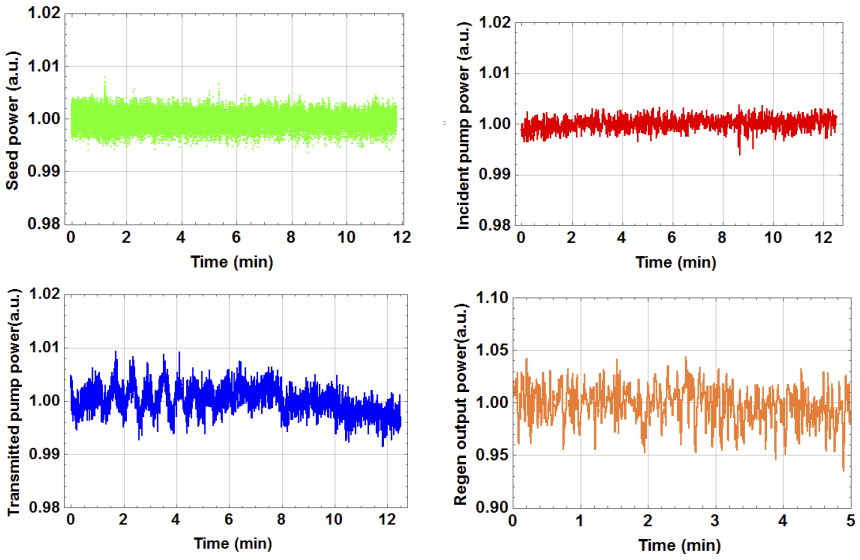

Fig. 8. Measured variation of (a) seed laser power, (b) incident pump power, (c) transmitted pump power and (d) Yb:YLF regenerative amplifier power. The regenerative amplifier data is taken at an output pulse energy of 16 mJ and at a pulse repetition rate of 2.5 kHz.

In closing, we present amplification data at 3.5 kHz (Fig. 9) and 10 kHz (Fig. 10) repetition rates. As discussed briefly above, 3.5 kHz was the highest repetition rate where we could achieve 20 mJ output pulse energy from the current system. Figure 9 shows the measured power efficiency of the Yb:YLF regenerative amplifier at 3.5 kHz, at round-trip numbers (n) of 71, 82 and 93. In all cases, the obtainable output power was limited due to the onset of thermal effects. The best performance (in terms of output energy/power) was achieved using 82 round-trips in the amplifier. In this case, we achieved an output power of 70 W at an absorbed pump power of around 460 W (incident power: 630 W). From the earlier cw-lasing experiments [1], we know that this operating regime is already pushing the thermal limits of the amplifier in terms of applicable incident/absorbed pump power. Since the extraction efficiency of the regenerative amplifier is

Optics EXPRESS

quite low compared to the laser, we expect stronger thermal effects. Similarly, Fig. 10 shows the regenerative amplifier performance at a repetition rate of 10 kHz. The system is pulse pumped by 50 µs long pulses (50% duty-cycle), and the amplifier produced pulses with up to 4.9 mJ energy after 150 round-trips, at an average absorbed power of 350 W (550 W average incident pump power, ~64% absorption). The corresponding average power of the system was around 47 W, leading to a conversion efficiency of 13.4%.

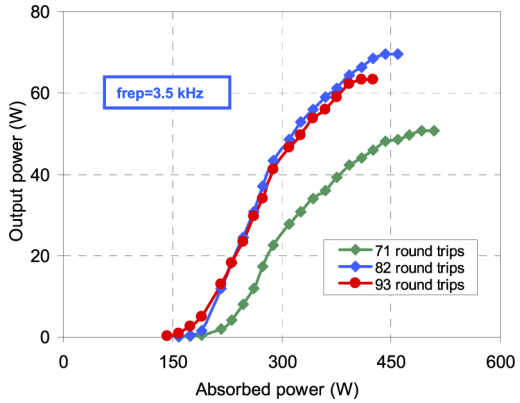

Fig. 9. Measured power performance of the Yb:YLF regenerative amplifier at 3.5 kHz repetition rate. The data is taken for cavity round-trips (n) of 71, 82 and 93.

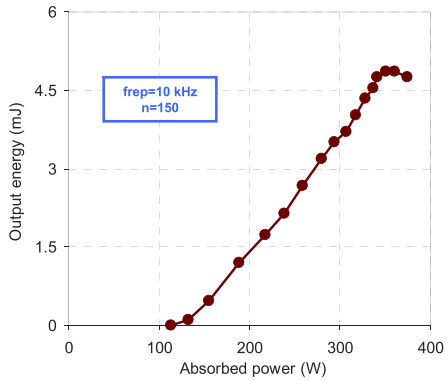

Fig. 10. Variation of regenerative amplifier output energy with absorbed pump power at a repetition rate of 10 kHz. The data is taken at a round-trip number (n) of 150.

To sum up, we have seen that due to thermal effects, the pump power that could be applied to the system in a safe manner is limited, which restricts the available gain per pulse at higher repetition rates. Once the gain per pulse decreases to the level of intracavity losses (which is measured to be 8% in the current system for the cold cavity), further increase in repetition rate is not possible. Note from Fig. 9 that, increasing the number of passes further does not allow better extraction, once the system is pushed to its limits. It is clear that minimization of passive losses of the system, could improve the performance of the Yb:YLF amplifier at higher repetition rates. As a more promising path, one can also improve the gain per pulse, by using a tighter spot size inside the crystal. However, as mentioned earlier, there one is limited by the LIDT of cavity optics. On the other hand, it is clear that, by using a seed source with broader bandwidth, the pulse lengths of the seed laser can be extended well above 1 ns stretched pulse duration. This in

Optics EXPRESS

turn should increase the effective damage threshold, and could enable operating the amplifier at higher fluence. Furthermore, one can also implement a dual-rod geometry, to boost the gain available from the system [39–41]. Hence, in future work, we are hoping to reach higher energies (>50 mJ) and output power levels (>250 W) from the next generation Yb:YLF regenerative amplifiers, by implementing a dual-rod cavity, and by employing a broader seed source with longer stretched pulses, which could then potentially also reduce the amplified pulse duration to below 250 fs.

4. Conclusions

In conclusion, to the best of our knowledge, we have presented the highest average power ever obtained from a Yb:YLF regenerative amplifier to date. Specifications of the amplifier such as pulse energy dynamics, time behavior, output beam profile, spectral profile and energy fluctuations have been discussed in detail. Possible paths for improvements in the near future has also been elaborated. Currently, the main limitation is the narrow seed spectrum available. Future work will focus on development of higher power and higher energy sub-250-femtosecond Yb:YLF amplifiers, for applications such as pumping of high energy and average power optical parametric amplifiers [42], spectral broadening and compression of high energy pulses and ultrafast x-ray generation [43,44].

Funding

Seventh Framework Programme (FP7) FP7/2007- 2013; European Research Council Synergy Grant (609920).

Acknowledgments

The authors acknowledge support from previous group members L. E. Zapata, K. Zapata for establishing the indium-bonding technology for YLF at CFEL-DESY and M. Hemmer for early Yb:YLF amplifier work. UD acknowledges support from BAGEP Award of the Bilim Akademisi.

Disclosures

The authors declare no conflicts of interest.

References

1. U. Demirbas, H. Cankaya, J. Thesinga, F. X. Kartner, and M. Pergament, "Efficient, diode-pumped, high-power (>300W) cryogenic Yb:YLF laser with broad-tunability (995-1020.5 nm): investigation of E//a-axis for lasing," Opt. Express **27**(25), 36562–36579 (2019).
2. X. Delen, Y. Zaouter, I. Martial, N. Aubry, J. Didierjean, C. Honninger, E. Mottay, F. Balembois, and P. Georges, "Yb:YAG single crystal fiber power amplifier for femtosecond sources," Opt. Lett. **38**(2), 109–111 (2013).
3. A. Giesen, H. Hugel, A. Voss, K. Wittig, U. Brauch, and H. Opower, "Scalable Concept for Diode-Pumped High-Power Solid-State Lasers," Appl. Phys. B **58**(5), 365–372 (1994).
4. A. Giesen and J. Speiser, "Fifteen years of work on thin-disk lasers: Results and scaling laws," IEEE J. Sel. Top. Quantum Electron. **13**(3), 598–609 (2007).
5. C. J. Saraceno, "Mode-locked thin-disk lasers and their potential application for high-power terahertz generation," J. Opt. **20**(4), 044010 (2018).
6. J. Brons, V. Pervak, D. Bauer, D. Sutter, O. Pronin, and F. Krausz, "Powerful 100-fs-scale Kerr-lens mode-locked thin-disk oscillator," Opt. Lett. **41**(15), 3567–3570 (2016).
7. T. Nubbemeyer, M. Kaumanns, M. Ueffing, M. Gorjan, A. Alismail, H. Fattahi, J. Brons, O. Pronin, H. G. Barros, Z. Major, T. Metzger, D. Sutter, and F. Krausz, "1 kW, 200 mJ picosecond thin-disk laser system," Opt. Lett. **42**(7), 1381–1384 (2017).
8. L. E. Zapata, H. Lin, A. L. Calendron, H. Cankaya, M. Hemmer, F. Reichert, W. R. Huang, E. Granados, K. H. Hong, and F. X. Kartner, "Cryogenic Yb:YAG composite-thin-disk for high energy and average power amplifiers," Opt. Lett. **40**(11), 2610–2613 (2015).
9. L. E. Zapata, F. Reichert, M. Hemmer, and F. X. Kartner, "250 W average power, 100 kHz repetition rate cryogenic Yb:YAG amplifier for OPCPA pumping," Opt. Lett. **41**(3), 492–495 (2016).

Optics EXPRESS

10. D. C. Brown, "The promise of cryogenic solid-state lasers," IEEE J. Sel. Top. Quantum Electron. **11**(3), 587–599 (2005).
11. T. Y. Fan, D. J. Ripin, R. L. Aggarwal, J. R. Ochoa, B. Chann, M. Tilleman, and J. Spitzberg, "Cryogenic Yb3+-doped solid-state lasers," IEEE J. Sel. Top. Quantum Electron. **13**(3), 448–459 (2007).
12. R. L. Aggarwal, D. J. Ripin, J. R. Ochoa, and T. Y. Fan, "Measurement of thermo-optic properties of Y3Al5O12, Lu3Al5O12, YAIO(3), LiYF4, LiLuF4, BaY2F8, KGd(WO4)(2), and KY(WO4)(2) laser crystals in the 80-300 K temperature range," J. Appl. Phys. **98**(10), 103514 (2005).
13. J. Kawanaka, K. Yamakawa, H. Nishioka, and K. Ueda, "Improved high-field laser characteristics of a diode-pumped Yb : LiYF4 crystal at low temperature," Opt. Express **10**(10), 455–460 (2002).
14. D. E. Miller, J. R. Ochoa, and T. Y. Fan, "Cryogenically cooled, 149 W, Q-switched, Yb:LiYF4 laser," Opt. Lett. **38**(20), 4260–4261 (2013).
15. A. Bensalah, Y. Guyot, M. Ito, A. Brenier, H. Sato, T. Fukuda, and G. Boulon, "Growth of Yb3+-doped YLiF4 laser crystal by the Czochralski method. Attempt of Yb3+ energy level assignment and estimation of the laser potentiality," Opt. Mater. **26**(4), 375–383 (2004).
16. A. Sugiyama, M. Katsurayama, Y. Anzai, and T. Tsuboi, "Spectroscopic properties of Yb doped YLF grown by a vertical Bridgman method," J. Alloys Compd. **408-412**, 780–783 (2006).
17. D. C. Brown, S. Tornegard, and J. Kolis, "Cryogenic nanosecond and picosecond high average and peak power (HAPP) pump lasers for ultrafast applications," High Power Laser Sci. Eng. **4**, e15 (2016).
18. J. Kawanaka, K. Yamakawa, H. Nishioka, and K. Ueda, "30-mJ, diode-pumped, chirped-pulse Yb : YLF regenerative amplifier," Opt. Lett. **28**(21), 2121–2123 (2003).
19. D. Rand, D. Miller, D. J. Ripin, and T. Y. Fan, "Cryogenic Yb3+-doped materials for pulsed solid-state laser applications [Invited]," Opt. Mater. Express **1**(3), 434–450 (2011).
20. D. E. Miller, L. E. Zapata, D. J. Ripin, and T. Y. Fan, "Sub-picosecond pulses at 100 W average power from a Yb:YLF chirped-pulse amplification system," Opt. Lett. **37**(13), 2700–2702 (2012).
21. J. Manni, D. Harris, and T. Y. Fan, "High-gain (43 dB), high-power (40 W), highly efficient multipass amplifier at 995 nm in Yb:LiYF4," Opt. Commun. **417**, 54–56 (2018).
22. H. Cankaya, U. Demirbas, Y. Hua, M. Hemmer, L. E. Zapata, M. Pergament, and F. X. Kärtner, "190-mJ Cryogenically-Cooled Yb:YLF Amplifier System at 1019.7 nm," OSA Continuum **2**(12), 3547–3553 (2019).
23. Y. Hua, W. Liu, M. Hemmer, L. E. Zapata, G. J. Zhou, D. N. Schimpf, T. Eidam, J. Limpert, A. Tunnermann, F. X. Kartner, and G. Q. Chang, "87-W 1018-nm Yb-fiber ultrafast seeding source for cryogenic Yb: yttrium lithium fluoride amplifier," Opt. Lett. **43**(8), 1686–1689 (2018).
24. J. Kawanaka, H. Nishioka, N. Inoue, and K. Ueda, "Tunable continuous-wave Yb : YLF laser operation with a diode-pumped chirped-pulse amplification system," Appl. Opt. **40**(21), 3542–3546 (2001).
25. L. E. Zapata, D. J. Ripin, and T. Y. Fan, "Power scaling of cryogenic Yb:LiYF4 lasers," Opt. Lett. **35**(11), 1854–1856 (2010).
26. K. Beil, S. T. Fredrich-Thornton, C. Kränkel, K. Petermann, D. Parisi, M. Tonelli, and G. Huber, "New thin disk laser materials: Yb:ScYLO and Yb:YLF," in *CLEO/Europe and EQEC* (2011), p. CA11_16.
27. N. Coluccelli, G. Galzerano, L. Bonelli, A. Toncelli, A. Di Lieto, M. Tonelli, and P. Laporta, "Room-temperature diode-pumped Yb3+-doped LiYF4 and KYF4 lasers," Appl. Phys. B **92**(4), 519–523 (2008).
28. W. Bolanos, F. Starecki, A. Braud, J. L. Doualan, R. Moncorge, and P. Camy, "2.8 W end-pumped Yb3+:LiYF4 waveguide laser," Opt. Lett. **38**(24), 5377–5380 (2013).
29. N. Ter-Gabrielan, V. Fromzel, T. Sanamyan, and M. Dubinskii, "Highly-efficient Q-switched Yb: YLF laser at 995 nm with a second harmonic conversion," Opt. Mater. Express **7**(7), 2396–2403 (2017).
30. M. Vannini, G. Toci, D. Alderighi, D. Parisi, F. Cornacchia, and M. Tonelli, "High efficiency room temperature laser emission in heavily doped Yb : YLF," Opt. Express **15**(13), 7994–8002 (2007).
31. D. Alderighi, A. Pirri, G. Toci, and M. Vannini, "Tunability enhancement of Yb:YLF based laser," Opt. Express **18**(3), 2236–2241 (2010).
32. A. Pirri, D. Alderighi, G. Toci, M. Vannini, M. Nikl, and H. Sato, "Direct Comparison of Yb3+:CaF2 and heavily doped Yb3+:YLF as laser media at room temperature," Opt. Express **17**(20), 18312–18319 (2009).
33. F. D. Lelii, S. Jun, F. Pirzio, G. Piccinno, M. Tonelli, and A. Agnesi, "Laser investigation of Yb:YLF crystals fabricated with the micro-pulling-down technique," Appl. Opt. **57**(9), 2223–2226 (2018).
34. J. G. Yin, Y. Hang, X. M. He, L. H. Zhang, C. C. Zhao, J. Gong, and P. X. Zhang, "Direct comparison of Yb3+-doped LiYF4 and LiLuF4 as laser media at room-temperature," Laser Phys. Lett. **9**(2), 126–130 (2012).
35. N. Coluccelli, G. Galzerano, L. Bonelli, A. Di Lieto, M. Tonelli, and P. Laporta, "Diode-pumped passively mode-locked Yb : YLF laser," Opt. Express **16**(5), 2922–2927 (2008).
36. F. Pirzio, L. Fregnani, A. Volpi, A. Di Lieto, M. Tonelli, and A. Agnesi, "87 fs pulse generation in a diode-pumped semiconductor saturable absorber mirror mode-locked Yb:YLF laser," Appl. Opt. **55**(16), 4414–4417 (2016).
37. H. Cankaya, U. Demirbas, M. Pergament, M. Hemmer, Y. Hua, L. E. Zapata, and F. X. Kärtner, "160-mJ Cryogenically-Cooled Yb:YLF Amplifier System at 1019 nm," in *CLEO Europe* (Munich, 2019).
38. A. L. Calendron, J. Meier, M. Hemmer, L. E. Zapata, F. Reichert, H. Cankaya, D. N. Schimpf, Y. Hua, G. Q. Chang, A. Kalaydzhyan, A. Fallahi, N. H. Matlis, and F. X. Kartner, "Laser system design for table-top X-ray light source," High Power Laser Sci. Eng. **6**, e12 (2018).

Optics EXPRESS

39. H. Vanherzeele, "Continuous Wave Dual Rod Nd-Ylf Laser with Dynamic Lensing Compensation," Appl. Opt. **28**(19), 4042–4044 (1989).
40. E. C. Honea, R. J. Beach, S. C. Mitchell, J. A. Skidmore, M. A. Emanuel, S. B. Sutton, S. A. Payne, P. V. Avizonis, R. S. Monroe, and D. G. Harris, "High-power dual-rod Yb : YAG laser," Opt. Lett. **25**(11), 805–807 (2000).
41. A. L. Calendron, H. Cankaya, and F. X. Kartner, "High-energy kHz Yb:KYW dual-crystal regenerative amplifier," Opt. Express **22**(20), 24752–24762 (2014).
42. H. Cankaya, A. L. Calendron, C. Zhou, S. H. Chia, O. D. Mucke, G. Cirmi, and F. X. Kartner, "40-(J passively CEP-stable seed source for ytterbium-based high-energy optical waveform synthesizers," Opt. Express **24**(22), 25169–25180 (2016).
43. D. F. Zhang, A. Fallahi, M. Hemmer, X. J. Wu, M. Fakhari, Y. Hua, H. Cankaya, A. L. Calendron, L. E. Zapata, N. H. Matlis, and F. X. Kartner, "Segmented terahertz electron accelerator and manipulator (STEAM)," Nat. Photonics **12**(6), 336–342 (2018).
44. D. F. Zhang, A. Fallahi, M. Hemmer, H. Ye, M. Fakhari, Y. Hua, H. Cankaya, A. L. Calendron, L. E. Zapata, N. H. Matlis, and F. X. Kartner, "Femtosecond phase control in high-field terahertz-driven ultrafast electron sources," Optica **6**(7), 872–877 (2019).